

# Iridium(I) and Rhodium(I) Cationic Complexes with Triphosphinocalix[6]arene Ligands: Dynamic Motion with Size-Selective Molecular Encapsulation

Yasushi Obora, Yun Kui Liu, Li Hong Jiang, Kazuhiro Takenaka, Makoto Tokunaga, and Yasushi Tsuji\*

Catalysis Research Center and Division of Chemistry, Graduate School of Science, Hokkaido University, and CREST, Japan Science and Technology Corporation (JST), Sapporo 001-0021, Japan

Received October 6, 2004

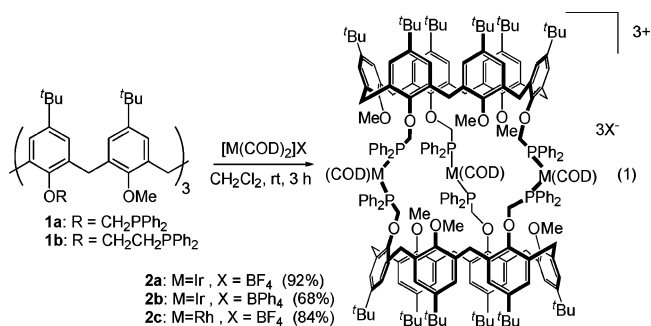
**Summary:** A novel capsule-shaped Ir(I) and Rh(I) cationic complexes with a triphosphinocalix[6]arene as a ligand were synthesized. These complexes showed dynamic behavior with size-selective molecular encapsulation, which was confirmed by variable-temperature  $^{31}\text{P}\{^1\text{H}\}$  NMR measurement in the presence of various molecules.

Calixarenes<sup>1</sup> are widely used template modules with well-defined cavities. Depending on the number of phenol rings involved, small (in calix[4]arene) to large cavities (such as in calix[8]arene) are provided. On the other hand, considerable attention has been paid to calixarenes possessing a phosphine functionality (so-called phosphinocalixarenes),<sup>2</sup> because they are unique phosphine ligands in transition-metal-catalyzed reactions.<sup>3</sup> In these reactions, most examples were limited to more accessible phosphinocalix[4]arenes,<sup>4</sup> although their cavities are too small to be utilized. In the present study, we prepared novel capsule-shaped<sup>5</sup> iridium(I) and rhodium(I) cationic complexes (**2**) with triphosphinocalix[6]arenes as multidentate ligands. Here we reveal that a combination of variable-temperature  $^{31}\text{P}\{^1\text{H}\}$  NMR and molecular modeling is a good probe to evaluate the size of an encapsulated molecule in the cavity during dynamic motion.

As a novel ligand, *p*-*tert*-butylcalix[6]arenes having three (diphenylphosphino)methyl (**1a**) or (diphenylphosphino)ethyl (**1b**) moieties were synthesized.  $^1\text{H}$ ,  $^{13}\text{C}\{^1\text{H}\}$ ,

and 2D-ROESY NMR spectra<sup>6</sup> at 25 °C showed that conformational interconversion of **1a** and **1b** was slow relative to the NMR time scale and these ligands have the cone structure in solution at 25 °C. X-ray crystallographic analysis<sup>6</sup> showed **1a** has a pinched-cone structure in the solid state.

Then, we reacted **1a** and **1b** with Ir(I) and Rh(I) cationic complexes. When **1a** was treated with  $[\text{Ir}(\text{COD})_2]^+\text{BF}_4^-$  in a 2:3 molar ratio at room temperature in  $\text{CH}_2\text{Cl}_2$  (7 mM) for 3 h, the novel iridium(I) cationic complex **2a** was obtained as a red solid in 92% yield (eq 1). Its ESI-MS spectrum and elemental analysis data



indicated that **2a** has three iridium metals and two calix[6]arene moieties. Under the present reaction conditions, no oligomers formed. Furthermore, even if **1a** and  $[\text{Ir}(\text{COD})_2]^+\text{BF}_4^-$  were allowed to react in a 1:1 molar ratio, **2a** was obtained in 85% yield (based on Ir) selectively without formation of oligomers or other

\* To whom correspondence should be addressed: Phone: +81-11-706-9155. Fax: +81-11-706-9156. E-mail: tsuji@cat.hokudai.ac.jp.

(1) (a) Gutsche, C. D. *Calixarenes Revisited: Monographs in Supramolecular Chemistry*; Stoddart, J. F., Ed.; The Royal Society of Chemistry: Cambridge, U.K., 1998. (b) *Calixarenes in Action*; Mandolini, L., Ungaro, R., Ed.; Imperial College Press: London, 2000. (c) *Calixarenes 2001*; Asfari, Z., Böhmer, V., Harrowfield, J., Vicens, J., Eds.; Kluwer Academic: Dordrecht, The Netherlands, 2001. (d) Rebek, J., Jr. *J. Chem. Commun.* **2000**, 637.

(2) (a) Wieser, C.; Dielman, C. B.; Matt, D. *Coord. Chem. Rev.* **1997**, *165*, 93. (b) Wieser-Jeunesse, C.; Matt, D.; Yaftian, M. R.; Burgard, M.; Harrowfield, J. M. C. *Acad. Sci. Paris, 11, Ser. IIC* **1998**, 479. (c) Neda, I.; Kaukorat, T.; Schmutzler, R. *Main Group Chem. News* **1998**, *6*, 4 and references therein.

(3) Collman, J. P.; Hegedus, L. S.; Norton, J. R.; Finke, R. G. *Principles and Applications of Organotransition Metal Chemistry*; University Science Books: Mill Valley, CA, 1987.

(4) (a) Takenaka, K.; Obora, Y.; Jiang, L.-H.; Tsuji, Y. *Organometallics* **2002**, *21*, 1158. (b) Takenaka, K.; Obora, Y.; Jiang, L.-H.; Tsuji, Y. *Bull. Chem. Soc. Jpn.* **2001**, *74*, 1709. (c) Plourde, F.; Gilbert, K.; Gagnon, J.; Harvey, P. D. *Organometallics* **2003**, *22*, 2862. (d) Lejeune, M.; Jeunesse, C.; Matt, D.; Kyrtsakas, N.; Welter, R.; Kintzinger, J.-P. *Dalton* **2002**, 1642. (e) Jeunesse, C.; Dieleman, C.; Steyer, S.; Matt, D. *Dalton* **2001**, 881 and references therein.

(5) For examples of molecular capsules, see: (a) Jacopozi, P.; Dalcanele, E. *Angew. Chem., Int. Ed.* **1997**, *36*, 613. (b) Ikeda, A.; Yoshimura, M.; Tani, F.; Naruta, Y.; Shinkai, S. *Chem. Lett.* **1998**, 587. (c) Ikeda, A.; Udzu, H.; Zhong, Z.; Shinkai, S.; Sakamoto, S.; Yamaguchi, K. *J. Am. Chem. Soc.* **2001**, *123*, 3872. (d) Conn, M. M.; Rebek, J., Jr. *Chem. Rev.* **1997**, *97*, 1647. (e) Hof, F.; Craig, S. L.; Nuckolls, C.; Rebek, J., Jr. *Angew. Chem., Int. Ed.* **2002**, *41*, 1488. (f) Corbellini, F.; Fiammengo, R.; Timmerman, P.; Crego-Calama, M.; Versluis, K.; Heck, A. J. R.; Luyten, I.; Reinhoudt, D. N. *J. Am. Chem. Soc.* **2002**, *124*, 6569. (g) Corbellini, F.; Di Costanzo, L.; Crego-Calama, M.; Geremia, S.; Reinhoudt, D. N. *J. Am. Chem. Soc.* **2003**, *125*, 9946. (h) Takeda, N.; Umamoto, K.; Yamaguchi, K.; Fujita, M. *Nature* **1999**, *398*, 794. (i) Olenyuk, B.; Whiteford, J. A.; Fechtenkötter, A.; Stang, P. *J. Nature* **1999**, *398*, 796. (j) Fochi, F.; Jacopozi, P.; Wegelius, E.; Rissanen, K.; Cozzini, P.; Marastoni, E.; Fiscaro, E.; Manini, P.; Fokkens, R.; Dalcanele, E. *J. Am. Chem. Soc.* **2001**, *123*, 7539. (k) Kang, J.; Rebek, J., Jr. *Nature* **1997**, *385*, 50. (l) Pinalli, R.; Cristini, V.; Sottili, V.; Geremia, S.; Campagnolo, M.; Caneschi, A.; Dalcanele, E. *J. Am. Chem. Soc.* **2004**, *126*, 6516. (m) Mecozzi, S.; Rebek, J., Jr. *Chem. Eur. J.* **1998**, *4*, 1016.

(6) See Supporting Information for details.

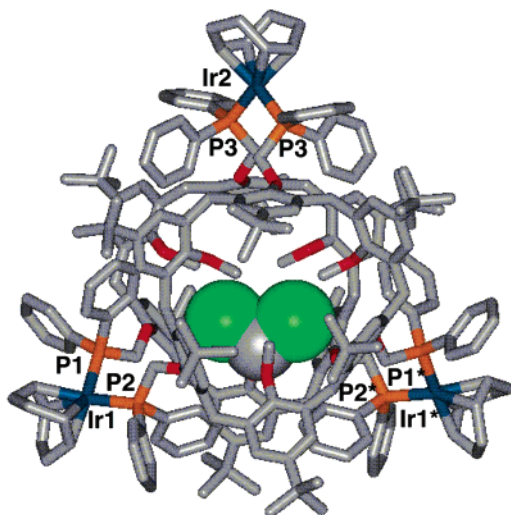


**Figure 1.** X-ray structure of the cationic part of **2a**. Hydrogen atoms are deleted for ease of viewing. The encapsulated  $\text{CH}_2\text{Cl}_2$  molecule is denoted as a space-filling model.

complexes of different calixarene/Ir compositions. Similarly,  $[\text{Ir}(\text{COD})_2]^+\text{BPh}_4^-$  and **1a** afforded **2b** in 68% yield. The Rh(I) complex  $[\text{Rh}(\text{COD})_2]^+\text{BF}_4^-$  also reacted with **1a** and afforded **2c** in 84% yield. In contrast, **1b**, having a (diphenylphosphino)ethyl moiety, did not react cleanly with  $[\text{Ir}(\text{COD})_2]^+\text{BF}_4^-$  and  $[\text{Rh}(\text{COD})_2]^+\text{BF}_4^-$  under the same conditions and only gave intractable mixtures of unidentified metal–phosphine complexes.

X-ray crystal analysis showed that **2a** has a capsule-shaped structure (Figure 1),<sup>7</sup> in which the calix[6]arene moiety adopted the same pinched-cone conformation as the free ligand **1a** (vide supra). The complex possesses an inner nanosized cavity with Ir–Ir distances of 14.6–14.9 Å. More importantly, Figure 1 clearly demonstrates that one  $\text{CH}_2\text{Cl}_2$  molecule is encapsulated in the cavity. As for the phosphines, the two Ir atoms (Ir1 and Ir1\* in Figure 1) possessed inequivalently cis-coordinated phosphines with different Ir–P distances (2.33 Å for Ir1–P1 and 2.38 Å for Ir1–P2). In contrast, the other Ir atom (Ir2 in Figure 1) was coordinated equivalently by cis phosphines with the same Ir–P distance (Ir2–P3 = 2.28 Å). Thus, **2a** has three inequivalent phosphorus atoms in a 1:1:1 ratio.

In solution, the  $^{31}\text{P}\{^1\text{H}\}$  NMR spectrum of **2a** in  $\text{CD}_2\text{Cl}_2$  (5 mM, 25 °C) showed one broad peak (a line width at half the maximum height of the resonance:  $\Delta\nu = 100$  Hz) at 16.3 ppm (Figure 2A). On the other hand, the NMR spectrum in  $\text{Cl}_2\text{CDCDCl}_2$  (5 mM, 25 °C) showed three  $^{31}\text{P}$  resonances at 15.3 (d,  $^2J(\text{P},\text{P}) = 18$  Hz), 15.9 (d,  $^2J(\text{P},\text{P}) = 18$  Hz), and 16.4 (s) ppm (Figure 2B). When the temperature was lowered to –60 °C, the spectrum shown in Figure 2A changed into one which showed three  $^{31}\text{P}$  resonances at 15.6 (d,  $^2J(\text{P},\text{P}) = 17$  Hz), 17.3 (s), and 18.5 ppm (d,  $^2J(\text{P},\text{P}) = 17$  Hz), similar to Figure 2B. These splitting patterns and the  $^2J(\text{P},\text{P})$  values indicated that there were three inequivalent P atoms in solution, and two of them were coupled to each other with inequivalently cis-coordinated geometry, as ob-

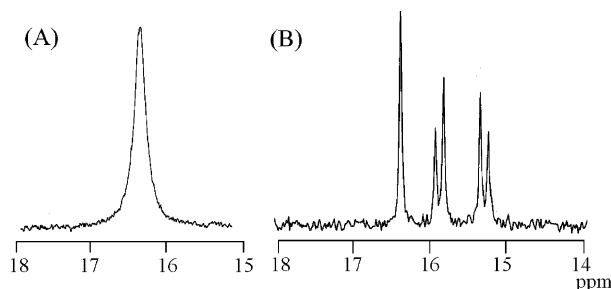


**Figure 2.**  $^{31}\text{P}\{^1\text{H}\}$  NMR spectra (162 MHz, 5 mM, 25 °C) of **2a** in (A)  $\text{CD}_2\text{Cl}_2$  and (B)  $\text{Cl}_2\text{CDCDCl}_2$ .

served in the X-ray structures of **2a** (Figure 1). At 65 °C, the spectrum of Figure 2B converged into one broad signal at 16.6 ppm ( $\Delta\nu = 298$  Hz). Activation enthalpies for these dynamic behaviors which equalized the three P atoms were determined by simulating these spectra at various temperatures:  $\Delta H^\ddagger = 27(1)$  kJ mol<sup>-1</sup> in  $\text{CD}_2\text{Cl}_2$  and 64(3) kJ mol<sup>-1</sup> in  $\text{Cl}_2\text{CDCDCl}_2$ .<sup>8</sup> During the dynamic behavior, the phosphine ligands did not dissociate, since  $^{31}\text{P}$  chemical shifts fell into the same range for  $[\text{Ir}(\text{DPPB})(\text{COD})]^+\text{BF}_4^-$  (15.2 ppm)<sup>9</sup> and no  $^{31}\text{P}$  resonances of free phosphine ligands appeared in the variable-temperature measurement. The rhodium analogue **2c** showed the same solvent-dependent spectra<sup>6</sup> as in Figure 2 at 25 °C: 26.0 ppm (d,  $^1J(\text{P},\text{Rh}) = 136$  Hz) in  $\text{CD}_2\text{Cl}_2$  and 24.8 (dd,  $^1J(\text{P},\text{Rh}) = 135$  Hz,  $^2J(\text{P},\text{P}) = 32$  Hz), 25.0 (dd,  $^1J(\text{P},\text{Rh}) = 135$  Hz,  $^2J(\text{P},\text{P}) = 32$  Hz), and 26.6 ppm (d,  $^1J(\text{P},\text{Rh}) = 135$  Hz) in  $\text{Cl}_2\text{CDCDCl}_2$ . In these cases, the  $^1J(\text{P},\text{Rh})$  coupling was permanently maintained, indicating that no dissociation of the phosphine ligands occurred.

The aforementioned results indicated that the dynamic motion of **2a** and **2c** in solution was dependent on the solvent size. Therefore, this phenomenon may be caused by size sensitivity inherent in the cavity of **2a** and **2c**. Thus, the  $^{31}\text{P}\{^1\text{H}\}$  NMR spectra of **2a** were measured in the presence of various organic molecules (30% v/v) in  $\text{CDCl}_3$  (5 mM, 25 °C) to investigate the sensitivity of the cavity (Table 1). Since **2a** has sparing solubility in the hydrocarbon molecules listed in Table 1, all the NMR measurements were performed with added  $\text{CDCl}_3$ . As a result, these molecules in Table 1 can be classified into three groups:<sup>10</sup> group A (entries 1–4), group B (entries 5–11), and group C (entries 12–15). We estimated the size of the molecules by two values. One is the Connolly solvent-excluded volume<sup>11a</sup> ( $V$ ) of structures optimized by B3LYP/6-31G(d,p) DFT calculations. The other is the maximum projection area<sup>6,12</sup> (A) of the solvent-accessible surface<sup>11b</sup> on the same DFT-optimized structure. Molecules in group A showed one broad  $^{31}\text{P}$  resonance having a significant variation of  $\Delta\nu$  values (197–315 Hz). Group B contains seven molecules that showed three different  $^{31}\text{P}$  resonances, indicating that the dynamic behaviors were

(8) In  $\text{CDCl}_3$  and  $\text{ClCD}_2\text{CD}_2\text{Cl}$  (5 mM),  $^{31}\text{P}\{^1\text{H}\}$  NMR of **2a** also showed one broad peak at 25 °C: 17.2 ppm ( $\Delta\nu = 188$  Hz) in  $\text{CDCl}_3$  and 17.4 ppm ( $\Delta\nu = 230$  Hz) in  $\text{ClCD}_2\text{CD}_2\text{Cl}$ . Variable-temperature  $^{31}\text{P}\{^1\text{H}\}$  NMR showed similar dynamic behavior in these solvents:  $\Delta H^\ddagger = 41(2)$  kJ mol<sup>-1</sup> in  $\text{CDCl}_3$  and 49(2) kJ mol<sup>-1</sup> in  $\text{ClCD}_2\text{CD}_2\text{Cl}$ .

(9) Chaloner, P. A. *J. Organomet. Chem.* **1984**, *266*, 191.

(10) The  $^{31}\text{P}\{^1\text{H}\}$  NMR spectra were insensitive to concentrations of molecules in the range of 30–70% v/v in  $\text{CDCl}_3$ .

(11) (a) Connolly, M. L. *J. Am. Chem. Soc.* **1985**, *107*, 1118. (b) Connolly, M. L. *Science* **1983**, *221*, 709.

(12) The area calculation was performed on a 0.07 Å gridded map.

(7) Crystal data: monoclinic, crystal dimensions 0.20 × 0.20 × 0.08 mm, space group  $C2$  (No. 5),  $a = 33.75(1)$  Å,  $b = 20.155(6)$  Å,  $c = 20.504(7)$  Å,  $\beta = 117.045(3)^\circ$ ,  $V = 12422(7)$  Å<sup>3</sup>,  $Z = 2$ ,  $D_{\text{calcd}} = 1.239$  g cm<sup>-3</sup>,  $T = -160$  °C,  $\mu = 17.73$  cm<sup>-1</sup>,  $R = 0.062$ ,  $R_w = 0.076$ , GOF = 1.505.

**Table 1.**  $^{31}\text{P}\{^1\text{H}\}$  NMR of **2a** with Various Molecules<sup>a</sup>

group	entry	molecule	$^{31}\text{P}$ resonance/ppm	$V^b/\text{\AA}^3$	$A^c/\text{\AA}^2$
A	1	$\text{CH}_2\text{Cl}_2$	16.9 ( $\Delta\nu = 197$ Hz)	52.9	35.9
	2	$\text{ClCH}_2\text{CH}_2\text{Cl}$	17.1 ( $\Delta\nu = 238$ Hz)	70.2	40.9
	3	$\text{CHCl}_3$	17.3 ( $\Delta\nu = 210$ Hz)	67.7	42.0
	4	$\text{CCl}_4$	17.0 ( $\Delta\nu = 315$ Hz)	80.5	42.2
B	5	$\text{Cl}_2\text{CHCHCl}_2$	16.7 (d, $J = 17$ Hz), 17.2 (d), 17.8 (s)	100.3	49.5
	6	2,3-dimethyl-2-butene	16.7 (d, $J = 17$ Hz), 17.2 (s), 17.3 (d)	92.0	57.0
	7	$\text{Br}_2\text{CHCHBr}_2$	16.9 (d, $J = 17$ Hz), 17.2 (d), 18.2 (s)	(122.2)	57.0
	8	benzene	17.1 (d, $J = 17$ Hz), 17.6 (s), 17.8 (d)	(71.0)	60.4
	9	toluene	17.2 (d, $J = 17$ Hz), 18.0 (s), 18.1 (d)	87.6	62.1
	10	<i>o</i> -xylene	17.5 (d, $J = 18$ Hz), 18.1 (s), 18.2 (d)	103.9	66.7
	11	<i>m</i> -xylene	17.4 (d, $J = 18$ Hz), 18.1 (s), 18.2 (d)	104.2	67.2
C	12	cumene	17.7 ( $\Delta\nu = 216$ Hz)	123.1	68.1
	13	<i>p</i> -xylene	17.8 ( $\Delta\nu = 212$ Hz)	105.6	69.0
	14	mesitylene	17.2 ( $\Delta\nu = 218$ Hz)	122.0	78.1
	15	5- <i>tert</i> -butyl- <i>m</i> -xylene	17.4 ( $\Delta\nu = 214$ Hz)	176.3	83.1

<sup>a</sup> **2a** (5 mM) in the presence of the molecule (30% v/v) in  $\text{CDCl}_3$  at 25 °C. <sup>b</sup> Connolly solvent-excluded volume. <sup>c</sup> Maximum projection area of the solvent-accessible surface.

sufficiently slow on the NMR time scale at 25 °C. The molecules in group C showed one broad  $^{31}\text{P}$  resonance, but with comparable  $\Delta\nu$  values (212–218 Hz). Roughly, these groups could be categorized by  $V$  (group A,  $V < 81 \text{ \AA}^3$ ; group B,  $V = 81\text{--}105 \text{ \AA}^3$ ; group C,  $V > 105 \text{ \AA}^3$ ), but there are two exceptions in group B:  $\text{Br}_2\text{CHCHBr}_2$  and benzene (entries 7 and 8). More appropriately,  $A$  is a good measure to characterize the molecules (group A,  $A < 45 \text{ \AA}^2$ ; group B,  $A = 45\text{--}68 \text{ \AA}^2$ ; group C,  $A > 68 \text{ \AA}^2$ ), which is quite reasonable, assuming that the molecules were captured along the plane determined by the three metals inside the cavity, as shown in the X-ray structures of **2a** (Figure 1) and **2c**.<sup>13</sup> The rhodium analogue **2c** also showed molecule-sensitive dynamic behavior<sup>6</sup> similar to that in Table 1. The molecules in group A

may be too small to fit the cavity of **2** and cannot restrict the dynamic behavior at 25 °C. The molecules in group B just fit in the cavity and slow the dynamic behavior. The molecules in group C are too large to enter the cavity.<sup>14</sup> Therefore, the cavity of **2a** was accommodated with  $\text{CDCl}_3$  in the measurement and resulted in a similar dynamic motion to have comparable  $\Delta\nu$  values.

**Acknowledgment.** Y.O. and Y.K.L. contributed equally to this work.

**Supporting Information Available:** Text, figures, and tables giving experimental procedures and spectroscopic data for **1** and **2** and measurements of  $V$  and  $A$  and CIF files giving crystallographic data for **1a** and **2a**. This material is available free of charge via the Internet at <http://pubs.acs.org>.

OM049227J

(13) The X-ray analysis was done for **2c**.<sup>6</sup> The atom connecting scheme and inclusion of one  $\text{Cl}_2\text{CHCHCl}_2$  molecule into the cavity of **2c** have been confirmed. However, the  $R$  value did not converge to an acceptable level, due to considerable disorder of solvents outside the cavity. The molecular structure is shown in the Supporting Information (Figure S2).

(14) NMR spectra of **2a** and **2c** in deuterated group C molecules might be very interesting. Unfortunately, however, the solubility of the complexes in these hydrocarbon molecules is very poor.